文章编号:1672-3961(2009)03-0031-06

# Power system inter-area oscillation damping control with FACTS devices

CAO Gang[1], DONG Zhao-yang[2*], WONG Kit-po[2], XUE Yu-sheng[3]
(1.Transgrid, NSW, Australia; 2. Department of Electrical Engineering, Hong Kong Polytechnic University, Hong Kong;
3. Nanjing Automation Research Institute, Nanjing 210003, China)

**Abstract**: Various control schemes have been developed to solve the power system inter-area oscillation problem. Increasingly Flexible AC Transmission Systems (FACTS) devices are being planned to solve various power system operational and planning problems in some large-scale power systems in many countries. One of the design objectives is to reduce some critical inter-area oscillations existing in the system. In this paper, FACTS controllers, based on variable structure control technology, were proposed to alleviate the interarea oscillation problem. Both series and parallel connected FACTS devices were studied. Case studies were presented to illustrate the effectiveness of the proposed controllers.

**Key words**: FACTS; inter-area oscillation; power system stability and control

# 应用 FACTS 装置实现电力系统区间震荡阻尼控制

曹刚[1],董朝阳[2*],黄洁宝[2],薛禹胜[3]
(1. 越网公司,新南威尔士, 澳大利亚; 2. 香港理工大学电机工程学系, 香港;
3. 中国南京自动化研究院, 江苏 南京 210003)

**摘要**:为了解决电力系统区间震荡问题, 已经发展形成了多种控制策略.在许多国家一些大规模的电力系统中,为解决各种不同的电力系统的运行和规划问题,采用了越来越多的柔性交流输电系统装置(FACTS).设计目标之一是减少系统中存在的一些临界区间震荡.基于变结构控制技术,提出了 FACTS 控制器,用以缓解区间震荡问题,研究了串联和并联的 FACTS 装置,并给出实例加以研究用以说明所提出控制器的有效性.

**关键词**:柔性交流输电系统;区间震荡;电力系统稳定性和控制
**中图分类号**:TM712 **文献标志码**:A

## 0 Introduction

Power systems have been increasingly interconnected over the past decades. Together with the corresponding complexity of the interconnected power system, the stressed transmission system has made system inter-area oscillations attracting more and more attentions from system operators. A typical oscillation, once started, may continue for a while and then disappear by the damping toque from the system, or if there is no sufficient damping, continue to grow and cause system instability through losing synchronism. Inter-area oscillations have become one of the major design objectives in system operations and planning with many transmission network service providers (TNSPs). Some of the inter-area damping control can be realized by flexible AC transmission system (FACTS) devices such as Static Var Compensators (SVCs)[1], although the primary objective of FACTS devices is to control power flow and improve transmission capability in steady state[2].

The electromechanical oscillation appears in a power

**Received date**: 2009-05-04

**Biography**: CAO Gang(1971-), male, born in Shanghai, Ph.D., Operations Engineer, his main research interests include power systems stability and control. E-mail: gang@itee.uq.edu.au

**Corresponding author**: DONG Zhao-yang(1971-), male, born in Shanxi, Associate Professor, his research interest includes power system planning, power system security, electricity market, and computational intelligence & its application in electric power engineering. E-mail: eezydong@polyu.edu.hk

system due to the interactions among the system components. Most of the oscillation modes are generator rotors swing against each other. The oscillation normally occurs in the frequency range of 0.2 HZ to 2.5 HZ[2]. The inter-area oscillations, which are typically in the lower frequency range of 0.2 HZ to 1 HZ, are exhibited as one group of machines swing relative to other groups. The inter-area oscillations usually appear in the system involving several groups interconnected by a relatively weak transmission line with heavy power transfers. Compared with lower frequency, the higher frequency oscillation modes typically involve one or more generators swinging against the rest of the power system, which is referred to as local mode oscillation[3].

The oscillations stability analysis and control is an important and active topic in power system research and applications. In the past, power system stabilizer (PSS) is recognized as an efficient and economical method to damp oscillations[2-3]. In recent years, as a new solution, various FACTS controllers have been developed for damping of power system oscillations[4-5]. Based on the control theory applied, the presented controllers can be divided to two groups: linear controllers and nonlinear controllers. In linear control, the system dynamics are linearized around the pre-selected system operating point according to Lyapunov's linearization method. The linearized system is an approximation of the original system at the operating point. Therefore, these controllers suffer from the performance degeneracy problem when system operating point deviates from the pre-designed point. Nonlinear control techniques can provide more effective control of power systems due to their capability to handle nonlinear operating characteristics. There are already some researches on nonlinear FACTS controller design for damping power system oscillations in recent years. The Feedback Linearization (FL) method has been used in FACTS controller design in [5]. Energy based Control Lyapunov Function Method (CLF) had been successfully applied in series FACTS devices controller in [4]. The adaptive control is used in FACTS controller design in [6]. The $H_\infty$ control is also successfully applied in TCSC controller to damp inter-area oscillations in [7]. In [8], fuzzy control technique is applied in FACTS controller design. These nonlinear controllers have good performance if the system model is accurate and the parameters are precisely obtained; however the robustness of these controllers is not guaranteed in the presence of modeling inaccuracies, i.e. parameter uncertainty and un-modeled dynamics, especially in FL method. The distinguished feature of Variable structure control (VSC)[9-10] is, under certain conditions, the sliding mode of a VSC is invariant with respect to system perturbations and external disturbances. As a robust control technique, VSC has been widely used in nonlinear control design. In the last decade, VSC has been applied in power system control[11]. In [12], VSC based controller is used to adjust the series capacitor capacity and the braking resistors to improve transient stability based on the SMIB case. In [5], feedback liberalization combined with VSC controller is applied to design power system stabilizer. The VSC based SVC controller is used to damping inter-area oscillations in [13]. In this paper, the nonlinear series TCSC controller based on the sliding control theory is developed to increase damping of system inter-area oscillations. The performance of developed controller is verified by example case.

## 1 Variable structure control

In FACTS controller design, line resistance is usually ignored and simple machine models is used to reduce the problem complexity. However, this model's imprecision has a strong effect on controller performance. The imprecision normally includes the uncertainty caused by the simplified representation of system dynamics and system disturbance. The variable structure control is recognized as a powerful robust control technique to deal with this model uncertainty.

The basic idea of VSC is to drive any state of the control system outside the switching surface to reach the surface in a finite time. After reaching the surface, the system follows the designed system dynamics to a stable equilibrium point. During the control process, the structure of the control system varies according to the designed reaching law. Therefore, the main steps of design procedure include sliding surface definition and reaching law design. The detailed VSC theory can be found in [9-10].

For a control system represented in (1), the basic procedure of the VSC-based controller design includes following steps. The first step is a notational simplification, which allows the nth order problems to be replaced by an

equivalent first order problem. We define this first order system model as a controllable form, which is shown in (2).

$$\dot{x} = A(x) + B(x)\mu, \tag{1}$$

$$\begin{aligned} \dot{x}_1 &= x_2, \\ \dot{x}_2 &= x_3, \\ &\cdots \\ \dot{x}_{n-1} &= x_n, \\ x_n &= \alpha(x) + \beta(x)\mu. \end{aligned} \tag{2}$$

The sliding surface in the state-space $\mathbf{R}^n$ can be defined as the following equation.

$$S(x) = \boldsymbol{C}^{\mathrm{T}} x = C_1 x_1 + C_2 x_2 + \cdots + C_{n-1} x_{n-1} + x_n, \tag{3}$$

where $\boldsymbol{C} = [\, C_1 \quad C_2 \quad \cdots \quad C_n \,]$ and $C_n = 1$.

Based on (3), by substituting $x_i$ with $\frac{\mathrm{d}^{i-1}}{\mathrm{d}t} x_1$, $i = 1, 2, \cdots, n$, we have the following equation.

$$\left( \frac{\mathrm{d}^{n-1}}{\mathrm{d}t} + C_{n-1} \frac{\mathrm{d}^{n-2}}{\mathrm{d}t} + \cdots + C_2 \frac{\mathrm{d}}{\mathrm{d}t} + C_1 \right) x_1 = 0. \tag{4}$$

Then, we transfer (4) to eigenvalue form as (5)

$$(p - \lambda_1)(p - \lambda_2) \cdots (p - \lambda_n) = 0. \tag{5}$$

The eigenvalues of (5) are chosen at the left side of the phase plane to make the sliding mode in the sliding surface asymptotically stable. By expanding (5) and comparing it with (4), the constants $C_1, C_2, \cdots, C_n$ can be evaluated. It is important to note that the sliding equation (3) is independent of the system parameters, which is why the VSC is invariant in respect to system perturbation and external disturbances[10,14]

Another important step is reaching condition definition ($S\dot{S} \leqslant 0$). The popular reaching condition can be defined as(6)[10], . Based on this reaching condition, the reaching law can be defined as[14](7)

$$\begin{aligned} \dot{S} &< 0 \quad when \quad S > 0, \\ \dot{S} &= 0 \quad when \quad S = 0, \\ \dot{S} &> 0 \quad when \quad S < 0, \end{aligned} \tag{6}$$

$$\dot{S} = -KS - Q\,\mathrm{sgn}(S), \tag{7}$$

where $K$ and $Q$ are both positive constants and Sign function $\mathrm{sgn}(S)$ is defined as

$$\mathrm{sgn}(S) = \begin{cases} 1, & S > 0; \\ 0, & S = 0; \\ -1, & S < 0. \end{cases} \tag{8}$$

After the switching surface and reaching laws are properly designed, the control algorithm can be proposed by a differential the sliding surface equation (3) and combined with reaching law equation (8). We have:

$$\begin{aligned} \dot{S}(x) &= C_1 \dot{x}_1 + C_2 \dot{x}_2 + \cdots + C_{n-1} \dot{x}_{n-1} + \dot{x}_n = \\ &C_1 x_2 + C_2 x_3 + \cdots + C_{n-1} x_n + \dot{x}_n = \\ &C_1 x_2 + C_2 x_3 + \cdots + C_{n-1} x_n + \alpha(x) + \\ &\beta(x)\mu = -KS - Q\,\mathrm{sgn}(S). \end{aligned} \tag{9}$$

Obviously, the control algorithm is derived as

$$\begin{aligned} \mu = \frac{1}{\beta(x)} ( &-KS - Q\,\mathrm{sgn}(S) - C_1 x_2 - \\ &C_2 x_3 - \cdots - C_{n-1} x_n ). \end{aligned} \tag{10}$$

During the control design, an ideal sliding mode is difficult to obtain due to the sampling mechanism and system delay. We can observe the chattering control signal generated by the sign function $\mathrm{sgn}(S)$ especially near the equilibrium point. This high-frequency discontinuous signal should be replaced by smoother signals. A simple and widely used method is by using the saturation function $\mathrm{Sat}(S/\phi)$ instead of $\mathrm{sgn}(S)$ in reaching law (7)[10,16], where

$$sat\left( \frac{S}{\phi} \right) = \begin{cases} \mathrm{sgn}\left( \frac{s}{\phi} \right), & \left| \frac{s}{\phi} \right| \geqslant 1; \\ \frac{s}{\phi}, & \left| \frac{s}{\phi} \right| < 1. \end{cases} \tag{11}$$

## 2　TCSC model and controller design

The basic principle of TCSC is to compensate the inductive voltage drop in the line by an inserted capacitance to control the effective reactance of the transmission line. For transmission lines involving TCSC, the TCSC can be modeled as a variable reactance as shown in Figure 1 (a)[15]. Its injection model is shown as in (b), where:

$$P_{si} = \mu_{CSC} \frac{1}{X_L} V_i V_j \sin\theta_{ij}, \tag{12}$$

$$P_{sj} = -P_{si}, \tag{13}$$

$$\mu_{CSC} = \frac{X_C}{X_L - X_C}. \tag{14}$$

The control output limitations are:

$$\mu_{\min} < \mu_{CSC} < \mu_{\max}, \tag{15}$$

where $\mu_{\min} = \frac{X_{C\min}}{X_L - X_{C\min}}$, $\mu_{\max} = \frac{X_{C\max}}{X_L - X_{C\max}}$.

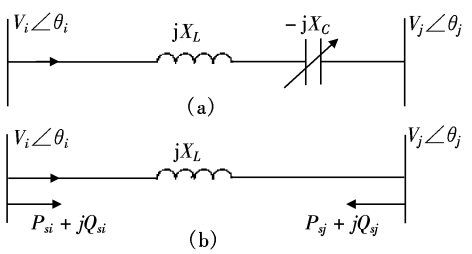


Fig.1　TCSC injection model

With the defined injection model, the two-area sys-

tem dynamic equations with TCSC installed can be expressed as:

$$\dot{\delta} = \omega,$$
$$\dot{\omega} = \omega_0 \Delta P_m - \frac{\omega_0}{M_{eq}} \frac{V_1 V_2}{X_L} \sin\delta (1 + \mu_{CSC}) + e(t), \tag{16}$$

where $\delta = \delta_1 - \delta_2$, $\omega = \omega_1 - \omega_2$.

Let

$$F = \omega_0 \Delta P_m,$$
$$G = \frac{\omega_0}{M_{eq}} \frac{V_1 V_2}{X_L}. \tag{17}$$

The system dynamic equation can be expressed in the form:

$$\dot{\omega} = F - G\sin\delta - G\sin\delta \mu_{CSC} + e(t). \tag{18}$$

The control objective is to make the relative oscillation between the two areas to be zero. Therefore, speed deviation is chosen as the system control state. Thus, the sliding surface can be designed as:

$$S = k\omega = 0,$$
$$\dot{S} = k\dot{\omega} = k(F - G\sin\delta - G\sin\delta \mu_{CSC} + e(t)), \tag{19}$$

where $k$ is a positive constant.

Similar as before, the reaching law is defined as in (20) to eliminate chattering.

$$\dot{S} = -KS - QSat\left(\frac{S}{\phi}\right) = \sigma. \tag{20}$$

Finally, combining (19) and (20), the control law can be defined as:

$$\mu_{CSC} = \frac{1}{G\sin\delta}\left(F - G\sin\delta + \frac{Q}{k} Sat\left(\frac{S}{\phi}\right) + \frac{K}{k} S\right), \tag{21}$$

where $Q/k$ is chosen to be greater than the magnitude of the uncertainty $e(t)$. The control output $\mu_{CSC}$ is limited by the operating limitation of TCSC as defined in (15).

In controller (21), $F$ is a constant, $K$, $Q$ and $k$ are positive control gains. The only unknown variable is $\delta$, which can be estimated by the same method as in shunt controller design.

Controller (21) can be further designed for both angle differences and speed oscillation control, which means the angle difference between two areas can be controlled at a desired value when system oscillation is damped out under a revised TCSC controller. To achieve this control objective, the sliding surface should be modified to be:

$$S = k_1(\delta - \delta_S) + k_2\omega, \tag{22}$$

where $\delta_S$ is a designed post-fault equilibrium angle difference. Then, we have:

$$\dot{S} = k_1\dot{\delta} + k_2\dot{\omega} =$$
$$k_1\omega + k_2(F - G\sin\delta - G\sin\delta\mu_{CSC} + e(t)). \tag{23}$$

By similar procedure, the new controller can be designed as:

$$\mu_{CSC} = \frac{1}{G\sin\delta}\left(\frac{k_1}{k_2}\omega + F - G\sin\delta + \frac{Q}{k_2} Sat\left(\frac{S}{\phi}\right) + \frac{K}{k_2} S\right). \tag{24}$$

## 3 Case studies

A typical two-area power system with a series connected FACTS device is illustrated in Figure 2[3]. The generators are considered in a two axis model with AVR control.

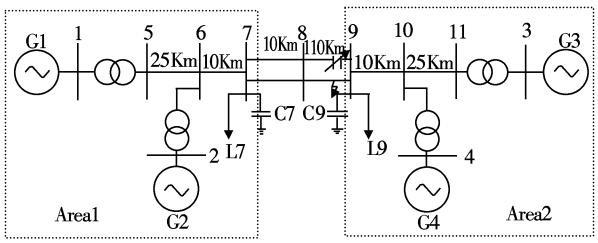


Fig.2 Classical two-area four-machine system with TCSC

The basic configuration of the system includes two areas which are connected through long transmission lines (two circuits). Two local loads and fixed shunt capacitive compensators are connected at Bus 7 and Bus 9 respectively.

Under steady states, 400 MW active power is transmitted from Area 1 to Area 2. The simulated fault sequence is as follows: a three phase fault occurs at one line from Bus 8 to Bus 9 close to Bus 9 and this fault is cleared by opening the breaker of the faulted line (fault happened at 1.5 s, cleared at $t = 1.6$ s). Followed by the fault and tripping action, the line impedance between Bus 7 and Bus 9 is altered, which causes power oscillation. The system has four generators, according the eigenvalue analysis in [16]; the system has three oscillation modes, one inter-area mode in which generators in Area 1 oscillate against generators in Area 2, and two local oscillation modes including one in which Generator 1 oscillates against Generator 2 and another in which Generator 3 oscillates against Generator 4. In this paper, damping the speed difference between two centers of inertia $\omega_{COI1} - \omega_{COI2}$ is chosen as the control objective.

The TCSC device is located at the un-faulted circuit from Bus 8 to Bus 9. The proposed control law is applied to adjust the capacitance of the inserted TCSC to add damping for inter-area mode oscillation. The controller

parameters are chosen as $\phi = 0.5$, $K = 2$, $Q = 5$, $\mu_{max} = 0.35$ and $\mu_{min} = -0.15$. The original percentage compensation of TCSC at a steady state is set to 0 percent. The control results of relative rotor angle and velocity between two areas COI during the whole control process are shown in Figure 3. The solid line is performance with the TCSC controller and dashed line is without control. The oscillation frequency is approximately $f = 0.55$ Hz. Obviously, the results show that inter-area oscillation can be damped within 5 seconds. Since the TCSC is settled down in a new operating condition, the inter-area phase angle is finally in a status different with the system response without control.

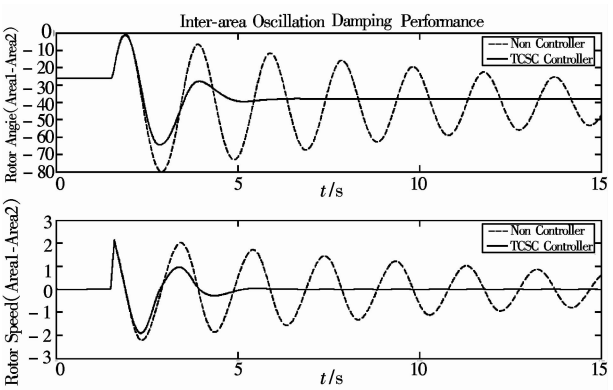


Fig.3　Simulation results (two-area four-machine system)-TCSC

Figure 4 shows that the power flow oscillation between two areas has been effectively damped by controller action. The performance is similar to speed oscillation damping. The TCSC compensation level is finally settled down at $\mu_{CSC} = 0.056$. Its output is given in Figure 5.

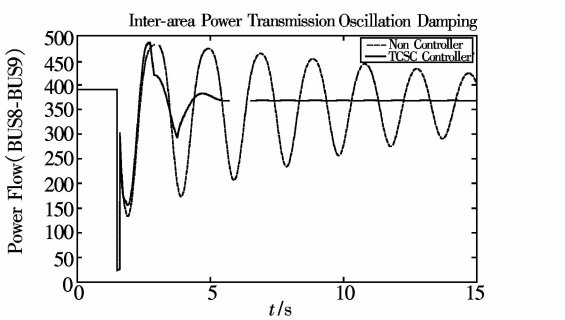


Fig.4　Power transmission curve (two-area four-machine system)-TCSC

TCSC in this case study is mainly designed for damping inter-area oscillation mode, so the other two local modes are not the primary objective. Figure 6 shows machine speed difference, where the oscillation frequency for local mode ($\omega_1 - \omega_2$) is around $f = 1.1$ Hz. The magnitude of the local mode oscillation is very small compared with the inter-area mode. As shown in the figure, the designed TCSC controller has a minor effect on local mode oscillation compared with the inter-area mode ($\omega_1 - \omega_3$).

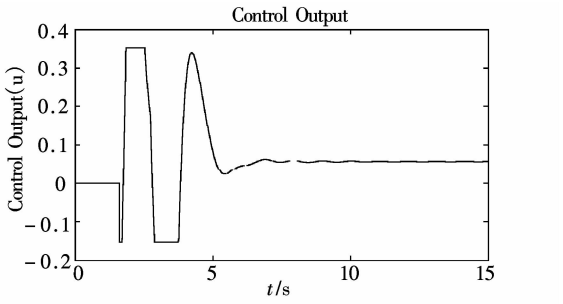


Fig.5　Control output (two-area four-machine system)-TCSC

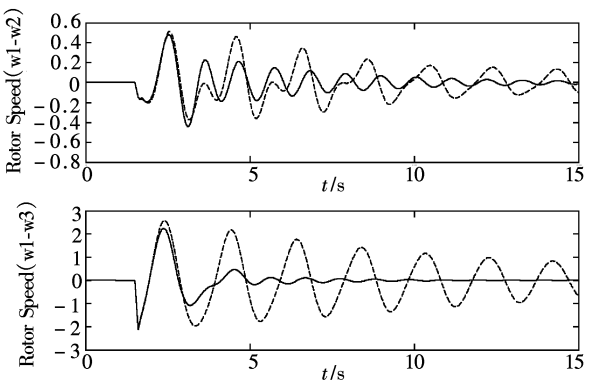


Fig.6　Speed oscillation between machines (two-area four-machine system)-TCSC

To verify the robust performance of the designed controller, various operation status and fault types are simulated. The first case is the load at Bus 7 increased 200 kW to 1 167 kW and load at Bus 9 decreased to 1 567 kW. Under the revised operating condition, the transferred power from Area 1 to Area 2 is reduced to 200 kW. The same fault sequence is tested with the same controller parameters as the previous simulation. The angle and speed oscillation damping results are shown in Figures 7 and 8. As shown in Figure 7 and 8, oscillation is damped out within five seconds after the fault is cleared, which is longer than the previous result. As the principle described in previous controller design process, the damping result is related with the power flow in the line where TCSC is connected. In case of heavy power flow, $\Delta P_e$ has a wider controllable range compared with light flow. Consequently, controller has better performance, which is shown with a shorter damping time in the first simulation result.

Another test is for a different fault type. A various fault type, mechanical power surge, is applied to test the controller's robust performance. In this case, the mechanical input of machines in Area 1 was suddenly increased 20

percent at $t = 1.5$ s and went back to normal at $t = 1.6$ s. The oscillation occurred following the actions. The TCSC controller with unaltered parameters was used to test the performance.

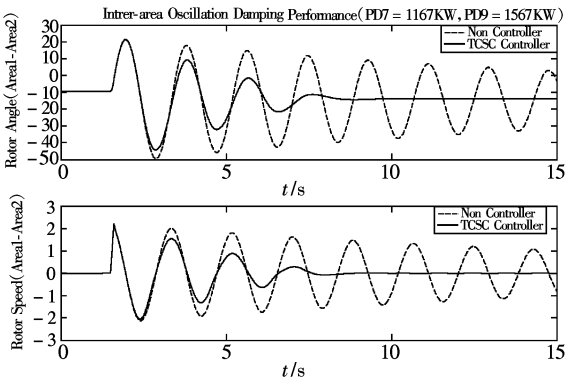


Fig.7 Robust performance (light power flow) TCSC

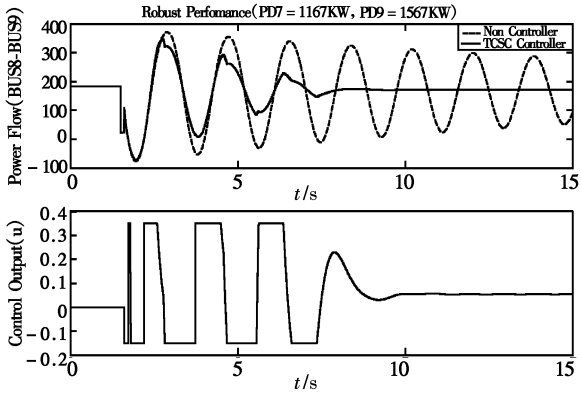


Fig.8 Robust performance in light power flow (power flow and control output)-TCSC

Figure 9 shows system angle and speed response after the fault. Obviously, oscillation is effectively damped, which can prove the robust performance of the designed TCSC controller. The corresponding control output and power flow oscillation damping are shown in Figure 10. Since the system is back to its original status, the controller output finally settled down at the same value as pre-fault $\mu_{CSC} = 0$.

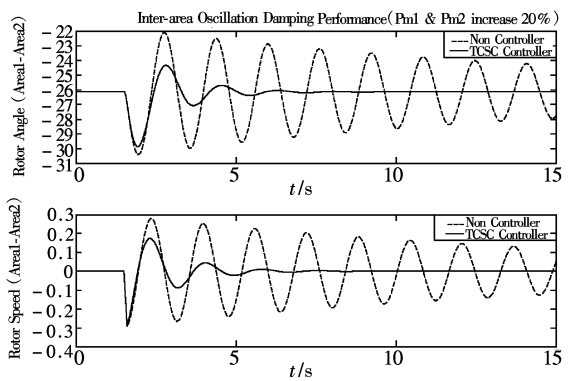


Fig.9 Robust performance ($P_m$ fault)-TCSC

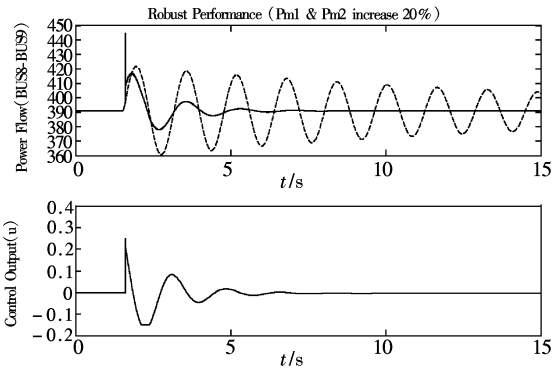


Fig.10 Robust performance for Pm fault (control output and power flow curve)- TCSC

## 4 Conclusion

More and more FACTS devices are being installed in the power systems for various operational and planning purposes. With the increasing inter-area oscillations observed in many power systems worldwide, damping of such undesirable oscillations has become one of the main controller design objectives in planning for FACTS devices in a power system. In this paper, a variable structure control based design approach is presented for damping power system inter-area oscillations with FACTS devices. TCSC is used as an illustrative FACTS device to show the effectiveness of the proposed controller. It provides some useful information for the system operators and planners in their planning practice with FACTS devices.

**Reference:**

[1] Powerlink Queensland Limited[EB/OL]. www.powerlink.com.au, 2009-05-01.

[2] SONG Y H, JOHNS A T. Flexible AC transmission systems (FACTS)[M]. London, England: The Institution of Electrical Engineers, 1999.

[3] KUNDUR P. Power system stability and control[M]. New York: McGraw Hill, 1994.

[4] NOROOZIAN M, GHANDHARI M, ANDERSSON G, et al. A robust control strategy for shunt and series reactive compensators to damp electromechanical oscillations[J]. IEEE Transactions on Power Delivery, 2001, 16:812-817.

[5] TAN Y L, WANG Y. Design of series and shunt FACTS controller using adaptive nonlinear coordinated design techniques [J]. IEEE Transactions on Power Systems, 1997, 12(3): 1374-1379.

[6] WU Q H, JIANG L. Nonlinear adaptive co-ordinated control of multimachine power systems[J]. Transactions of the Institute of Measurement and Control, 2002(24):195-213.

[7] MAJUMDER R, PAL B C, DUFOUR C, et al. Design and re-

altime implementation of robust FACTS controller for damping inter-area oscillation[J]. IEEE Transactions on Power Systems, 2006, 21(2):809-816.

[8] KAZEMI A, SOHRFOROUZANI M V. Power system damping using fuzzy controlled facts devices[J]. International Journal of Electrical Power and Energy Systems, 2006, 28:349-357.

[9] SLOTINE JJ E, LI W. Applied nonlinear control[M]. [S.l.]:Prentice Hall, 1991.

[10] GAO W, HUNG J C. Variable structure control: a survey [J]. IEEE Transactions on Industrial Electronics, 1993, 40: 2-22.

[11] DASH P K, SAHOO N C, DORAISWAMI R. A variable structure VAR stabilizer for power system control[J]. Electric Power Systems Research, 1993, 26:127-136.

[12] WANG Y, MOHLER R R, SPEE R, et al. Variable-structure FACTS controllers for power system transient stability[J]. IEEE Transactions on Power Systems, 1992, 7(1):307-313.

[13] POURBOGHRAT F, FARID F, HATZIADONIU C J, et al. Local sliding control for damping interarea power oscillations [J]. IEEE Transactions on Power Systems, 2004, 19(2): 1123-1134.

[14] ZHOU E Z. Application of static VAr compensators to increase power system damping[J]. Power Systems, IEEE Transactions on,1993, 8:655-661.

[15] CHIANG H D, THORP J S. The closest unstable equilibrium point method for power system dynamic security assessment [J]. IEEE Transactions on Circuits and Systems, 1989, 36: 1187-1200.

[16] PAI M A. Energy function analysis for power wystem stability [M]. [S.l.]: Kluwer Academic, 1989.

(编辑:胡春霞)